ORIGINAL ARTICLE

INTERNATIONAL JOURNAL OF RESEARCH IN PHARMACEUTICAL SCIENCES

Published by JK Welfare & Pharmascope Foundation Journal Home Page: www.ijrps.com

Design and Synthesis of 3, 5-Diphenylpyrazole derivatives as Selective Estrogen Receptor Modulators

Pritam N. Dube*[1,2], Vivekanand A. Chatpalliwar[2], Yogita B. Thombare[3], Tushar N. Lokhande[3]

[1]Matoshri College of Pharmacy, Eklahare, Near Odhagaon, Nashik-422105, Maharashtra, India
[2]Shree Neminath Jain Brahmacharyashram (Gurukul) Shriman Sureshdada Jain College of Pharmacy, Neminagar, Chandwad, Nashik-423101, Maharashtra, India
[3]MGV's Pharmacy College, Panchvati, Nashik-422003, Maharashtra, India

Article History:

Received on: 23 Nov 2019
Revised on: 02 Jan 2020
Accepted on: 04 Jan 2020

Keywords:

Breast cancer,
Docking,
MCF-7,
Pyrazole,
SERM

ABSTRACT

This exploratory work encompasses synthetic chemistry to develop novel 3, 5-diphenylethanone derivatives compounds based on the medicinally relevant scaffold of pyrazole as that of standard SERM *i.e.* Tamoxifen and Raloxifene. Specific strategies for the synthesis of novel analogues were used and were subjected to modeling and docking studies for analyzing the ER subtype selectivity. The *in-silico* studies were conducted in order to attain a better insight into the interactions of these molecules with their target receptor in order to study their subtype selectivity and preferential binding site. The various orientations taken by ligands while binding the estrogen receptor-α were studied over 1ERR (PDB) using Schrodinger *Maestro* environments. The anti-cancer potential of these derivatives were evaluated in estrogen receptor-positive cell lines in an *in vitro* assay, exploring MCF-7 and Zr-75-1 cell lines. Amongst all, the derivatives that displaced promising anticancer activity (4-chloro substituted, compound 4b) were selectively screened for *in vivo* anti-cancer activity subjected to NMU administration mammary carcinoma in female Sprague-Dawley rat. As hormone estrogen has been largely implemented in the metastasis of breast cancer, it has become imperative to measure levels of the hormone in tumor-affected animals. The percentage of incidences, tumor latency, tumor burden, and tumor volume was measured after sacrificing the experimental animals.

*Corresponding Author

Name: Pritam N. Dube
Phone: +91-9503981237
Email: pritamdube@gmail.com

ISSN: 0975-7538

DOI: https://doi.org/10.26452/ijrps.v13i3.1778

Production and Hosted by

IJRPS | www.ijrps.com

INTRODUCTION

Breast malignancy is one of the leading causes of malignancy in women, both in the developed and the developing world. The report denotes alarmingly high figures for breast cancer incidence, published in 2019 by American Cancer Society [1], estimated around 271,270 new cases of breast malignancy and whereas 42,260 estimated deaths. A perturbing shift in the age of incidence has additionally been observed with incrementing number of adolescent females reporting positive for disease [2]. Over 70% of breast cancer cases reported are hormone receptor-positive. Albeit several chemotherapeutic agents are available in the clinical setting; their efficacy is challenged due to their poor ability to

differentiate between diseased and mundane tissue leading to severe side effects. Hormone receptor-positive breast cancers are categorized as ER+ and PR+ [3].

Selective Estrogen Receptor Modulators (SERM) are the therapeutic agents that target ER+ cancers are referred to as [4]. The treatment of both advanced and early estrogen receptor-positive breast malignancy include currently used Tamoxifen, second and third-generation SERM in both pre and post-menopausal women [5]. Long-term treatment with available SERM is well-kenned to have rigorous side effects [6]. This has engendered considerable interest to identify incipient chemical entities that can be utilized for targeted therapy [7–9].

The scope of this research paper was to explore 3,5-diphenyl pyrazole derivatives as possible selective estrogen receptor modulators.

SERM are therapeutic agents that elicit anticancer activity by targeting the ER [10]. The net agonist or antagonist effect is the cumulative effect of several factors. Firstly, the critical components that govern ER action regard the structure of the ligand, its stereochemistry and the corresponding conformation of the ligand-receptor complex (post ligand binding). Secondly, ER action is also governed by the selectivity of the ligand interaction for the ER subtypes ERα and ERβ. Thirdly, the differential tissue concentration of the ER subtypes governs the tissue-specific effects of SERM. Finally, the receptor conformation post ligand binding plays a key role in the recruitment of a complex array of effectors components which include co-regulatory proteins that determine the transcriptional response of ER.

Clearly, the ligand structure and preference for ER subtypes can be considered as the first checkpoint towards the discovery to new leads that may possibly exhibit SERM activity.

This exploratory work encompasses synthetic chemistry to develop new compounds based on a medicinally relevant scaffold of pyrazole, as depicted in Figure 1. Specific strategies for the synthesis of novel analogues were used and were subjected to modeling and docking studies for analyzing the ER subtype selectivity. The computational studies were conducted in order to achieve a better insight into the interactions of these molecules with their target receptor in order to study their subtype selectivity and preferential binding site. The anti-cancer potential of these derivatives were evaluated in ERα and ERβ cell lines in an *in vitro* assay, exploring MCF-7 and Zr-75-1 cell lines [11]. Amongst all, the derivatives that displaced promising anticancer activity were selectively screened for *in vivo* anti-cancer activity subjected to NMU administration mammary carcinoma in female Sprague-Dawley rats [12].

As hormone estrogen has been largely implemented in the metastasis of breast cancer, it has become imperative to measure levels of the hormone in tumor-affected animals. The tumor latency, burden, and volume was measured after sacrificing the experimental animals. Figure 2

MATERIALS AND METHODS

Chemistry

AR/LR grade reagents were used after purifying and drying appropriately. Characterizations of the designed compounds are cited in the individual description. Melting points were measured using electrical melting point apparatus by open capillaries and were uncorrected [7].

The yield of respective processes are mentioned in parentheses following the m. p. of respective derivatives. Silica gel G plates activated at 110 °C for 30 min were used for TLC, developed using the solvent system: (a) Chloroform: Ethyl acetate (3:7); (b) Benzene: Methanol (4:1); (c) Benzene: Methanol (9:1), and are enclosed in parentheses herein during individual characterization of the compound.

The developed TLC plates were examined for colored spots that were apparent on exposing them to iodine vapors. The R_f values of purified compounds are represented herein individual characterization.

Single spot TLC, using various solvent systems, ascertained the purity of the compounds. Percentage yields shown are approximate along with the solvent used for crystallization in the case of solid compounds and are mentioned within brackets after the melting point (m. p.) reported in °C. IR spectra of all synthesized compounds were recorded on *JASCO* FT-IR 4000 spectrophotometer using KBr as a diluent and are expressed herein cm^{-1}.

The ^{1}H NMR spectra were recorded on *Bruker Avance* (400 *MHz*) Spectrometer in $CDCl_3$ solutions, whereas and ^{13}C NMR spectra were recorded with 100 *MHz* on the same facility. Chemical shifts (δ) in ppm are mentioned along with coupling frequencies; Mass spectra were recorded on a *Varian Inc*, 410 *Prostar Binary LC* with 500 MS IT PDA Detectors.

Method

The derivatives described as 2a-2g and 3a-3g are synthesized by the methods reported by Dube *et al*. 2016. [13].

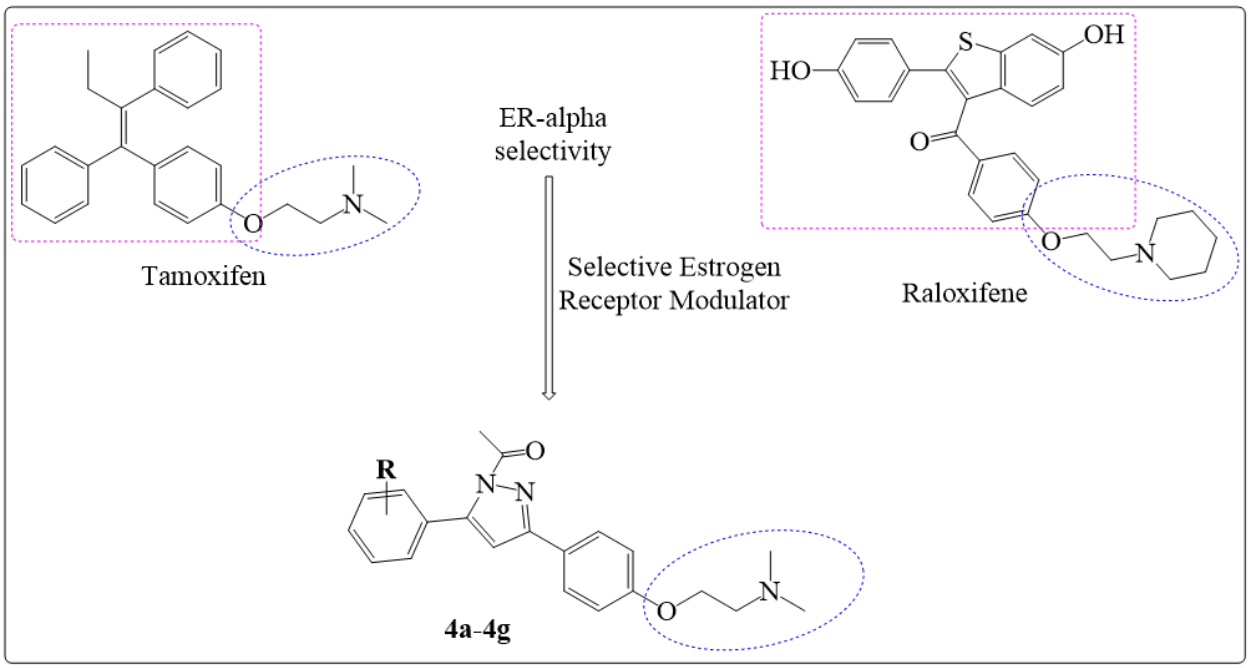

Figure 1: Pharmacophore design of 3, 5-diphenylethanone compounds (4a-4g)

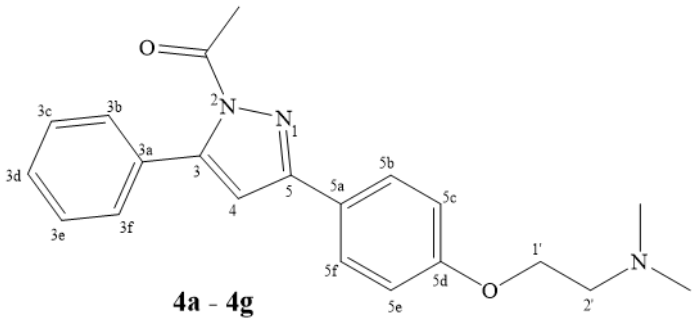

Figure 2: Structure and numerical assignment ofsynthesized derivatives

Synthesis of 1-(3-(4-(2-(dimethylamino)ethoxy)phenyl)-5-phenyl-1*H*-pyrazol-1-yl)ethan-1-one derivatives (4a-4g)

A mixture of compounds 3a–g (3 g), acetic acid (20 mL) and 2-chloro-*N, N*-dimethylethan-1-amine hydrochloride (4) (18.72 mmol, 1.8 g), anhydrous potassium carbonate (52 mmol, 7.2 g) were subjected to refluxing with constant stirring for 24 h. TLC method was used to monitor the reaction progress.

After completion of the reaction, the reaction mixture was cooled to room temperature, quenched with ice-cold water and the final compound was extracted with $CHCl_3$.

Then the anhydrous magnesium sulfate was treated with organic phase and the solvent was evaporated in vacuo.

The obtained derivatives 4a-4g, were purified by column chromatography on silica gel employing 30:1 $CHCl_3$-MeOH as eluent.

1-[3-(4-(2-(dimethylamino)ethoxy)phenyl)-5-phenyl-1*H*-pyrazol-1-yl]ethan-1-one (4a)

MP: 136-138°C (88.56); R_f: 0.58 (a); MW: 349.45; MF: $C_{21}H_{23}N_3O_2$; IR (KBr): 681 (Ar-H), 1189 (C-O), 1342 (C-N), 1518 (C=C), 1726 (C=O) cm^{-1}; ^1H NMR (DMSO, 400MHz): δ= 7.7-7.5 (*m*, 5H, Ar-H), 7.2 (*m*, 2H, Ar-H_{5b}, H_{5f}), 6.8 (*m*, 2H, Ar-H_{5c}, H_{5e}), 4.0 (*t*, 2H, CH_2 at 1'), 3.6 (*s*, 1H, CH of pyrazole), 2.8 (*t*, 2H, CH_2 at 2'), 2.3 (*s*, 6H, CH_3-N), 1.9 (*s*, 3H, CH_3-C=O); ^{13}C NMR (DMSO, 100MHz): δ= 168.7 (C=O), 157.3 (C_{5d}), 151.7 (C_3), 136.4 (C_{3a}), 133.4 (C_{5a}), 131.1 (C_{3d}), 128.8 (C_{3c}, C_{3e}), 128.2 (C_{3b}, C_{3f}), 126.2 (C_{5b}, C_{5f}), 114.2 (C_{5c}, C_{5e}), 66.2 ($C_{1'}$), 65.9 (C_5), 60.5 ($C_{2'}$), 47.1, 47.0 (CH_3-N), 39.9 (C_4), 23.4 (CH_3-C=O); MS: *m/z* = 349.19 [M^+, 100%], 350.20 [M+1, 22.7%], 350.19 [M+1, 1.1%].

1-(5-(4-chlorophenyl)-3-(4-(2-(dimethylamino)ethoxy)phenyl)-1*H*-pyrazol-1-yl)ethan-1-one (4b)

MP: 148-150°C (82.22); R_f: 0.72 (b); MW: 383.16;

MF: $C_{21}H_{22}ClN_3O_2$; IR (KBr): 678 (Ar-H), 713 (C-Cl), 1185 (C-O), 1344 (C-N), 1522 (C=C), 1731 (C=O) cm^{-1}; ^1H NMR (DMSO, 400MHz): δ= 7.9-7.6 (*m*, 4H, Ar-H), 7.3 (*m*, 2H, Ar-H_{5b}, H_{5f}), 6.9 (*m*, 2H, Ar-H_{5c}, H_{5e}), 4.0 (*t*, 2H, CH_2 at 1'), 3.7 (*s*, 1H, CH of pyrazole), 2.8 (*t*, 2H, CH_2 at 2'), 2.3 (*s*, 6H, CH_3-N), 1.9 (*s*, 3H, CH_3-C=O); ^{13}C NMR (DMSO, 100MHz): δ= 169.8 (C=O), 159.1 (C_{5d}), 152.2 (C_3), 137.1 (C_{3d}-Cl), 136.6 (C_{3a}), 134.0 (C_{5a}), 129.2 (C_{3c}, C_{3e}), 128.3 (C_{3b}, C_{3f}), 126.6 (C_{5b}, C_{5f}), 114.9 (C_{5c}, C_{5e}), 68.1 ($C_{1'}$), 66.7 (C_5), 61.1 ($C_{2'}$), 47.8, 47.6 (CH_3-N), 40.1 (C_4), 24.1 (CH_3-C=O); MS: *m/z* = 383.16 [M^+, 100%], 384.15 [M+1, 1.1%], 385.16 [M+2, 2.5%].

1-(3-(4-(2-(dimethylamino)ethoxy)phenyl)-5-(4-methoxyphenyl)-1*H*-pyrazol-1-yl)ethan-1-one (4c)

MP: 162-164°C (79.84); R_f: 0.68 (c); MW: 379.21; MF: $C_{22}H_{25}N_3O_3$; IR (KBr): 682 (Ar-H), 1193 (C-O), 1204 (C-O), 1336 (C-N), 1528 (C=C), 1730 (C=O) cm^{-1}; ^1H NMR (DMSO, 400MHz): δ= 7.9-7.6 (*m*, 4H, Ar-H), 7.2 (*m*, 2H, Ar-H_{5b}, H_{5f}), 6.8 (*m*, 2H, Ar-H_{5c}, H_{5e}), 4.1 (*t*, 2H, CH_2 at 1'), 3.9 (*s*, 3H, OCH_3), 3.6 (*s*, 1H, CH of pyrazole), 2.9 (*t*, 2H, CH_2 at 2'), 2.3 (*s*, 6H, CH_3-N), 1.9 (*s*, 3H, CH_3-C=O); ^{13}C NMR (DMSO, 100MHz): δ= 169.4 (C=O), 162.2 (C_{3d}-OCH_3), 158.8 (C_{5d}), 151.7 (C_3), 137.1 (C_{3a}), 134.3 (C_{5a}), 129.5 (C_{3c}, C_{3e}), 128.4 (C_{3b}, C_{3f}), 126.4 (C_{5b}, C_{5f}), 113.2 (C_{5c}, C_{5e}), 68.4 ($C_{1'}$), 66.8 (C_5), 61.2 ($C_{2'}$), 55.2 (OCH_3), 47.7, 47.6 (CH_3-N), 40.0 (C_4), 24.1 (CH_3-C=O); MS: *m/z* = 379.21 [M^+, 100%], 380.20 [M+1, 1.1%].

1-(5-(2, 6-dichlorophenyl)-3-(4-(2-(dimethylamino)ethoxy)phenyl)-1*H*-pyrazol-1-yl)ethan-1-one (4d)

MP: 158-160°C (85.14); R_f: 0.70 (c); MW: 417.12; MF: $C_{21}H_{21}Cl_2N_3O_2$; IR (KBr): 691 (Ar-H), 718 (C-Cl), 1187 (C-O), 1346 (C-N), 1521 (C=C), 1736 (C=O) cm^{-1}; ^1H NMR (DMSO, 400MHz): δ= 7.9-7.5 (*m*, 3H, Ar-H), 7.2 (*m*, 2H, Ar-H_{5b}, H_{5f}), 6.9 (*m*, 2H, Ar-H_{5c}, H_{5e}), 4.0 (*t*, 2H, CH_2 at 1'), 3.6 (*s*, 1H, CH of pyrazol), 2.8 (*t*, 2H, CH_2 at 2'), 2.4 (*s*, 6H, CH_3-N), 1.8 (*s*, 3H, CH_3-C=O); ^{13}C NMR (DMSO, 100MHz): δ= 171.2 (C=O), 159.6 (C_{5d}), 152.2 (C_3), 137.4 ($C_{3b,3f}$-Cl), 136.6 (C_{3a}), 134.0 (C_{5a}), 130.1 (C_{3d}), 129.2 (C_{3c}, C_{3e}), 126.6 (C_{5b}, C_{5f}), 114.9 (C_{5c}, C_{5e}), 68.1 ($C_{1'}$), 66.7 (C_5), 61.1 ($C_{2'}$), 47.8, 47.6 (CH_3-N), 40.1 (C_4), 24.1 (CH_3-C=O); MS: *m/z* = 417.12 [M^+, 100%], 419.12 [M+2, 2.5%].

1-(5-(2, 4-dimethoxyphenyl)-3-(4-(2-(dimethylamino)ethoxy)phenyl)-1*H*-pyrazol-1-yl)ethan-1-one (4e)

MP: 172-174°C (78.38); R_f: 0.62 (b); MW: 409.22; MF: $C_{23}H_{27}N_3O_4$; IR (KBr): 683 (Ar-H), 1194 (C-O), 1205 (C-O), 1337 (C-N), 1531 (C=C), 1729 (C=O) cm^{-1}; ^1H NMR (DMSO, 400MHz): δ= 7.9-7.6 (*m*, 3H, Ar-H), 7.2 (*m*, 2H, Ar-H_{5b}, H_{5f}), 6.7 (*m*, 2H, Ar-H_{5c}, H_{5e}), 4.2 (*t*, 2H, CH_2 at 1'), 3.9, 3.8 (*s*, 6H, OCH_3), 3.7 (*s*, 1H, CH of pyrazole), 2.9 (*t*, 2H, CH_2 at 2'), 2.2 (*s*, 6H, CH_3-N), 1.8 (*s*, 3H, CH_3-C=O); ^{13}C NMR (DMSO, 100MHz): δ= 169.8 (C=O), 163.4 (C_{3d}-OCH_3), 161.6 (C_{3b}-OCH_3), 157.7 (C_{5d}), 151.4 (C_3), 137.8 (C_{3a}), 134.1 (C_{5a}), 129.3 (C_{3c}, C_{3e}), 128.9 (C_{3f}), 125.1 (C_{5b}, C_{5f}), 113.5 (C_{5c}, C_{5e}), 68.3 ($C_{1'}$), 66.7 (C_5), 61.3 ($C_{2'}$), 55.3, 55.2 (OCH_3), 47.7, 47.5 (CH_3-N), 40.1 (C_4), 24.2 (CH_3-C=O); MS: *m/z* = 409.22 [M^+, 100%], 410.21 [M+1, 1.1%].

1-(3-(4-(2-(dimethylamino)ethoxy)phenyl)-5-(2, 3, 4-trimethoxyphenyl)-1*H*-pyrazol-1-yl)ethan-1-one (4f)

MP: 166-168°C (82.54); R_f: 0.56 (a); MW: 439.23; MF: $C_{24}H_{29}N_3O_5$; IR (KBr): 677 (Ar-H), 1189 (C-O), 1252 (C-O), 1335 (C-N), 1528 (C=C), 1730 (C=O) cm^{-1}; ^1H NMR (DMSO, 400MHz): δ= 7.7 (*m*, 1H, C_{3f}-H), 7.3 (*m*, 2H, Ar-H_{5b}, H_{5f}), 6.7 (*m*, 2H, Ar-H_{5c}, H_{5e}), 6.5 (*m*, 1H, C_{3e}-H), 4.3 (*t*, 2H, CH_2 at 1'), 3.9, 3.8 (*s*, 6H, OCH_3), 3.6 (*s*, 1H, CH of pyrazole), 2.9 (*t*, 2H, CH_2 at 2'), 2.2 (*s*, 6H, CH_3-N), 1.8 (*s*, 3H, CH_3-C=O); ^{13}C NMR (DMSO, 100MHz): δ= 167.4 (C=O), 162.8 (C_{3d}-OCH_3), 160.2 (C_{3b}-OCH_3), 158.1 (C_{5d}), 152.3 (C_{3c}-OCH_3), 151.4 (C_3), 138.1 (C_{3a}), 135.5 (C_{5a}), 129.3 (C_{3e}), 128.5 (C_{3f}), 125.4 (C_{5b}, C_{5f}), 113.7 (C_{5c}, C_{5e}), 69.2 ($C_{1'}$), 66.5 (C_5), 61.7 ($C_{2'}$), 59.6, 55.2, 55.1 (OCH_3), 46.8, 46.7 (CH_3-N), 40.2 (C_4), 23.1 (CH_3-C=O); MS: *m/z* = 439.23 [M^+, 100%], 440.23 [M+1, 1%].

1-(3-(4-(2-(dimethylamino)ethoxy)phenyl)-5-(4-fluorophenyl)-1*H*-pyrazol-1-yl)ethan-1-one (4g)

MP: 140-142°C (79.68); R_f: 0.66 (b); MW: 367.19; MF: $C_{21}H_{22}FN_3O_2$; IR (KBr): 688 (Ar-H), 714 (C-F), 1179 (C-O), 1347 (C-N), 1526 (C=C), 1732 (C=O) cm^{-1}; ^1H NMR (DMSO, 400MHz): δ= 7.9-7.6 (*m*, 4H, Ar-H), 7.2 (*m*, 2H, Ar-H_{5b}, H_{5f}), 6.9 (*m*, 2H, Ar-H_{5c}, H_{5e}), 4.1 (*t*, 2H, CH_2 at 1'), 3.6 (*s*, 1H, CH of pyrazole), 2.9 (*t*, 2H, CH_2 at 2'), 2.4 (*s*, 6H, CH_3-N), 1.9 (*s*, 3H, CH_3-C=O); ^{13}C NMR (DMSO, 100MHz): δ= 168.4 (C=O), 159.3 (C_{5d}), 153.5 (C_3), 138.2 (C_{3d}-F), 136.8 (C_{3a}), 134.3 (C_{5a}), 129.4 (C_{3c}, C_{3e}), 129.4 (C_{3b}, C_{3f}), 127.5 (C_{5b}, C_{5f}), 115.0 (C_{5c}, C_{5e}), 68.2 ($C_{1'}$), 66.8 (C_5), 61.2 ($C_{2'}$), 47.8, 47.6 (CH_3-N), 41.4 (C_4), 24.8 (CH_3-C=O); MS: *m/z* = 367.19 [M^+, 100%], 368.18 [M+1, 1.1%].

BIOLOGICAL EVALUATION

In vitro

Anti-cancer tests were performed using SRB assay protocols [13–15].

In vivo

Animal experiments were approved by IAEC of the concerned centre. 35 days of aged female virgin SD rats were housed at 6 per cage, with access to standard diet and water *ab libitum* and maintained at 25±2 °C under 12 h dark/light cycles. Solutions of carcinogen, *N*-Nitroso-*N*-methylurea (NMU) (Sigma, USA) were prepared fresh immediately before administration to the animals, using 3% acetic acid, normal saline, and NMU to get carcinogenic solution 10mg/mL. Solutions equivalent to 50 mg NMU /Kg weight of animals were administered *i.p.* on the 50^{th} and 57^{th} day of age [16]. Animals were grouped to have six each and were as follows: Group I was negative control receiving only saline; Group II was positive experimental control receiving the carcinogenic solution. Group III – Group VI receiving Tamoxifen, 4b and vehicle Tween 80, respectively. Animals in respective groups received the drug and the 3, 5-diphenylpyrazole derivatives, 10 mg/Kg each in Tween 80, orally after a two-week induction period, once a day for six weeks. Animals in the intact control group and untreated NMU group were given vehicle (Tween 80) according to the experimental protocol. Regular weekly palpation was carried out until the detection of mammary tumors under light ether anesthesia [15, 16].

At the end of the experimental, the observations were scored as follows: The time taken since the day of challenge for the first incidence of the tumour was noted as Tumour Latency Period, number of tumors/rat as marked as Tumor Burden. Size of every tumour was recorded using a micrometer calliper, and volume was calculated using the formula $V = 4/3\ nr^3$, where *r* is half of the average diameter [15, 16].

Intermittently, blood samples were collected from those animals in fifth week since NMU challenge, *i.e.* at the start of the treatment period, and in the tenth week from a challenge, *i.e.* at the end of the treatment period, from retro-orbital plexus in blood collection tubes and were analyzed for estrogen level measurement. These were analyzed for estrogen levels by ELISA [17].

Molecular Docking studies

Simulations were performed using solutions provided by *Schrödinger* [18]. The aforementioned structures were constructed using *ACD Freeware* and converted into *.mol files, before transferring into *OPLS*. A three-dimensional crystal structure (PDB: 1ERR, Sequence identity 95 %) was obtained and a cavity grid was prepared using *GLIDE*. The three-dimensional structures in flexible modes (generated using *LigPrep*) were docked in the rigid grid of the protein. The study was carried out with and without bound-water molecules within 5 ´ vicinity of the cavity, whereas hydrogen bonds, ring interactions, π-π stacking were opted for the study. These studies were carried using the *Xtra Presicion* (XP) module of the Schrödinger software for scoring the energy minimum.

RESULTS AND DISCUSSION

Chemistry

The designed compounds (4a-4g) were synthesized by alkylation of the hydroxyl group (3a-g) with the 2-chloro-*N, N*-dimethylethan-1-amine Hydrochloride (4) in the presence of K_2CO_3 as shown in Scheme 1. The designed compounds were characterized by using FT-IR, ^{1}H-NMR, ^{13}C-NMR and LC-MS techniques that allowed elucidating of their structures.

Biological Evaluation

The synthesized compounds were tested for their *in vitro* ERα+ human breast carcinoma cell line (MCF-7 & Zr-75-1) anticancer activity using SRB assay. Cytotoxicity results of synthesized compounds with their LC_{50}, TGI and GI_{50} value on breast cancer cell lines are listed in Table 1. The concentration of candidate derivatives in μg/mL inhibiting 50 % of cancerous cell growth are expressed as GI_{50}, the concentration inhibiting total cancerous cell growth is expressed as TGI, and the concentration inducing cytocidal effect in 50 % population of cancerous cell is expressed as LC_{50}. The percentages of inhibition/cytocidal effects induced by them are calculated considering the effect of standard Tamoxifen as 100.

The derivatives 4b show the most potent activity amongst the lot. Derivative, 4b is 4-chloro substituted, whereas 4c compound contains 4-methoxy substitution. The di-halo substituted and trimethoxy substituted compounds shows very less cytocidal activity.

Oral administration of 4b to the laboratory animals induced with mammary carcinogenesis resulted in decreased incidences of the tumor, reduced tumour burden and tumour volume. The recorded observations are tabulated in Table 2. The data from tumor incidences were statistically analyzed by the Chi-Square test for the assessment of significance in protection against tumor occurrence. A difference of $P<0.05$ was considered significant in all cases. The Chi-square analysis indicated that drug/tamoxifen treatment exhibited significant anti-tumour activity [(d*f*= 13.37, 5), $P<0.0201$] against NMU (*N*-Nitroso-*N*-methyl urea)-induced breast tumour as observed by a reduction in the tumour incidences.

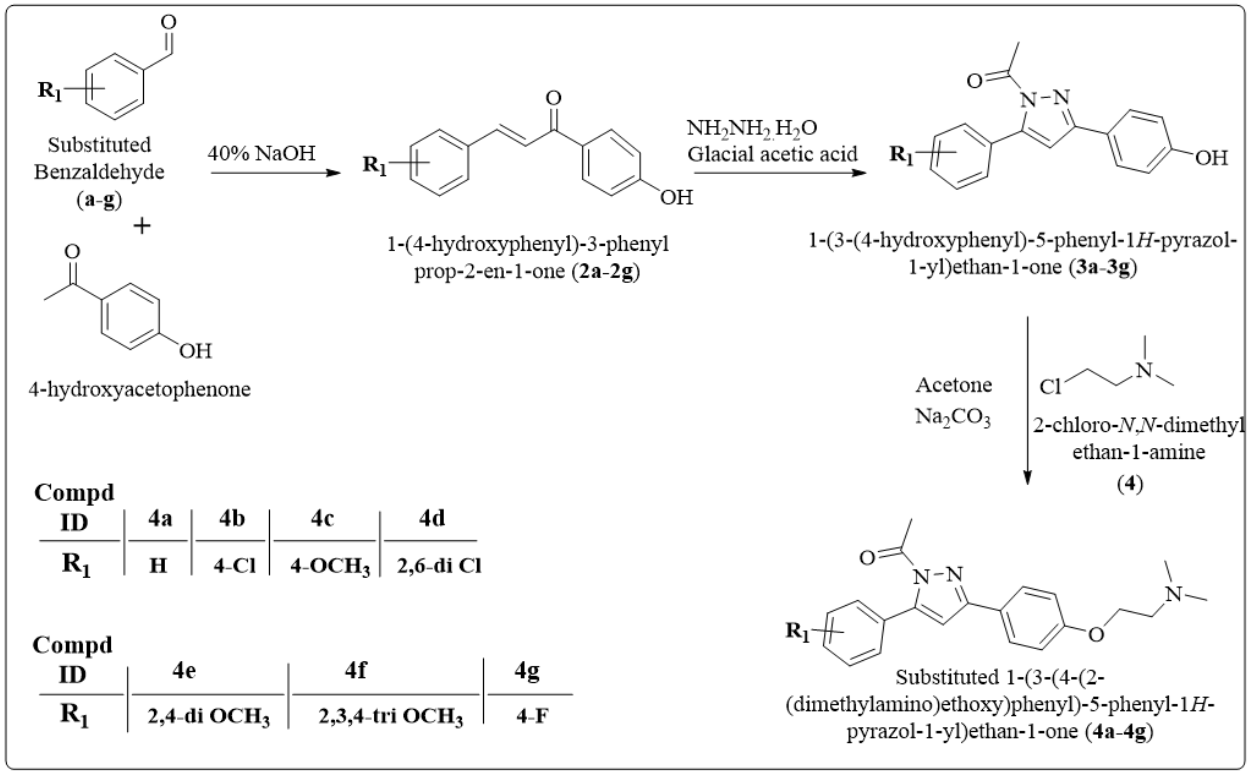

Compd ID	4a	4b	4c	4d
R_1	H	4-Cl	4-OCH_3	2,6-di Cl

Compd ID	4e	4f	4g
R_1	2,4-di OCH_3	2,3,4-tri OCH_3	4-F

Scheme 1: Synthetic path of designed 3, 5-diphenylpyrazole compounds

Table 1: *In-vitro* anticancer activity (μg/mL) ofsynthesized compounds

Sr. No.	MCF-7			ZR-75-1		
	LC_{50}a	TGI[b]	GI_{50}[c]	LC_{50}	TGI	GI_{50}
4a	94.2	66.4	30.4	>100	>100	42.1
4b	79.4	51.2	**20.8**	>100	>100	31.4
4c	66.8	42.8	**13.4**	>100	>100	23.5
4d	71.4	44.6	17.8	>100	>100	40.7
4e	69.5	74.6	25.1	>100	>100	37.3
4f	>100	81.3	37.8	>100	>100	56.5
4g	91.4	89.9	43.5	>100	>100	71.6
TAX	39.5	16.3	<10	>100	>100	<0.1

Bold text shows themost potent compound as compare to standard
^{TAM} tamoxifen
[a] 50% cytocidal effect produced by the concentration of compounds
[b] Total growth inhibition produced by the concentration of compounds
[c] 50% growth inhibition produced by the concentration of compounds

Table 2: Effect of treatment on mammary tumorigenesis

Group	Treatment	No. of rats with tumor	Incidences (%)	Tumor Latency (week)	Tumor burden	Tumor volume (mm^3)
I	MNU	6/6	100	4.1 ± 0.8	3.1 ± 0.14	4.8 ± 0.16
II	TAM	2/6	33.3	6.8 ± 0.3	6.2 ± 0.21	2.7 ± 0.11
III	4b	3/6	50	6.7 ± 0.3	6.4 ± 0.11	3.3 ± 0.14

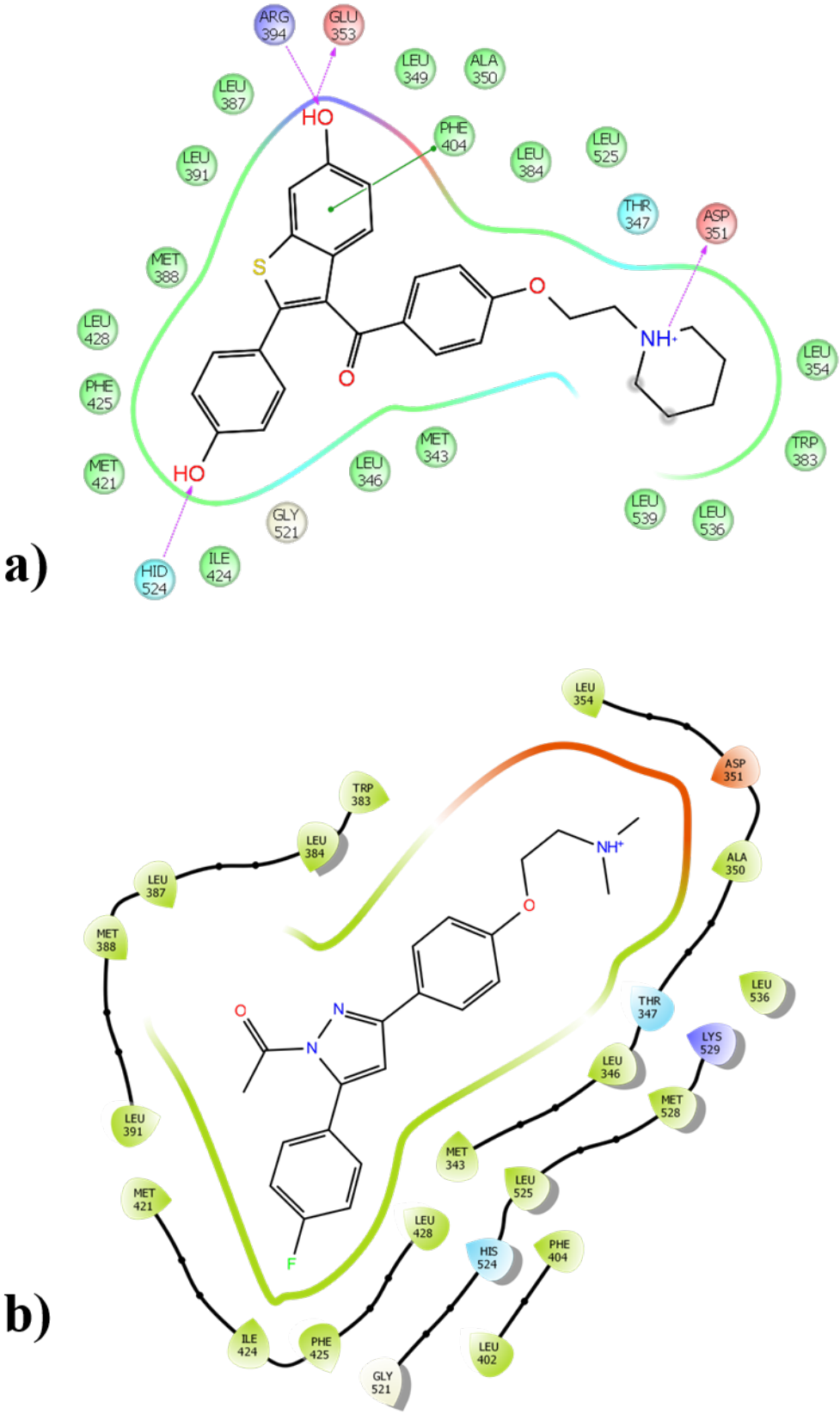

Figure 3: 2D Ligand Interaction diagram of (a)Raloxifen, (b) Compound 4g

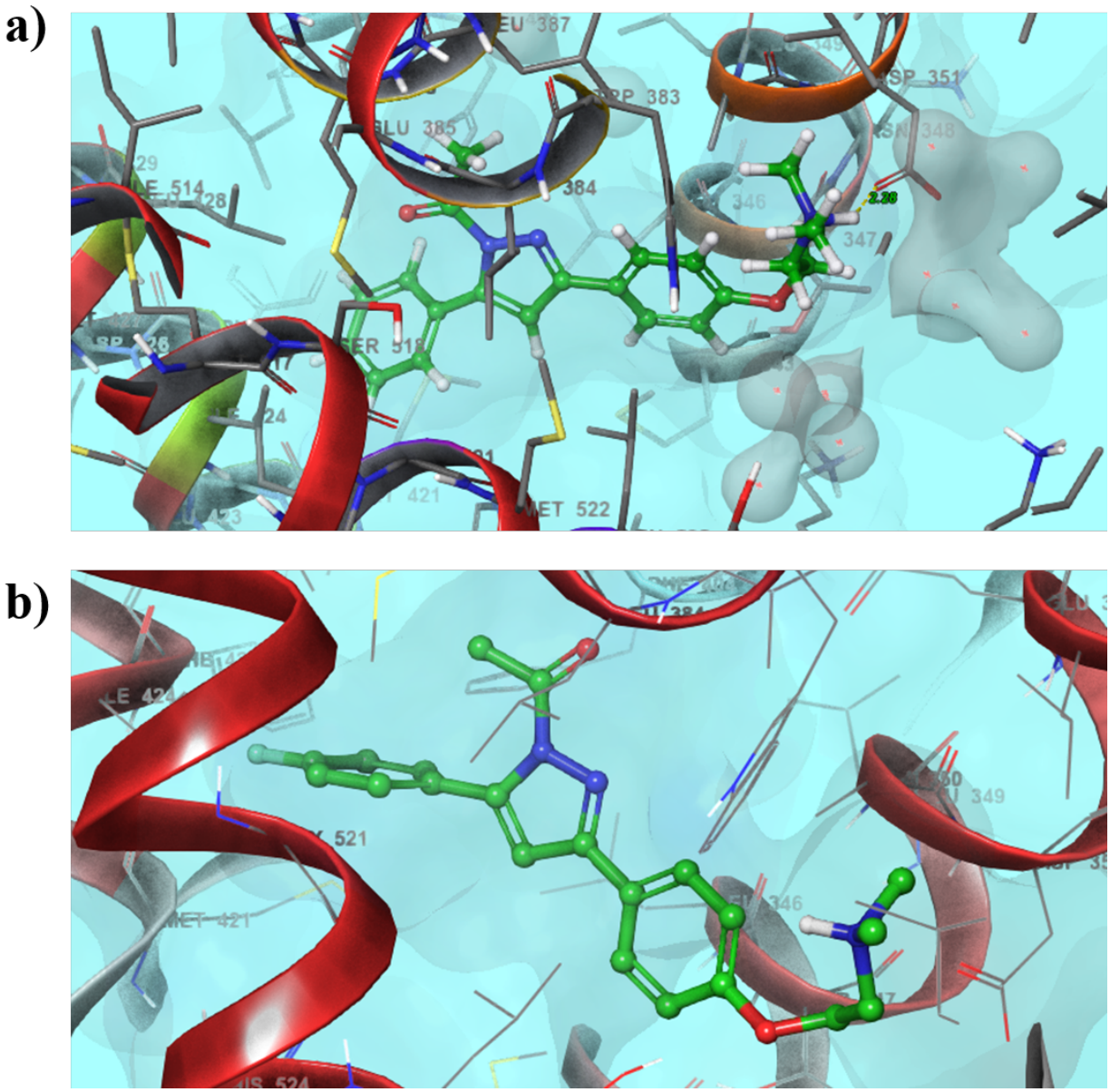

Figure 4: Docking analysis of (a) compound 4a and (b) compound 4b

Table 3: Estrogen levels (pg/mL) of animals on day 90

Group	Treatment	Estrogen level on 90^{th} Day (mean± SE)
I	Control	17.1±1.14
II	MNU	34.25±2.1
III	TAM	18.13±1.01
IV	4b	21.22±1.12

Corresponding to this, there was a reduction in the tumour volume (mm^3) in both groups.

Estrogen level of all groups with the control and NMU group were measured on the 90^{th} day since birth and observed for estrogen levels as given in Table 3.

The results show that compound 4b had a protuberant affinity towards estrogen receptors, similar to standard TAM.

Docking Study

The docking study was performed using Maestro-Glide and the results indicated acceptable trustworthiness of the parameters specified in reproducing the binding mode for synthesized compounds. After successful reproduction of the binding mode of RAL (Figure 3), the remaining data set were docked to search for the binding potentiality. Binding propensity was analyzed by docking on 1ERR, the crystal structure of ERα. It was observed that all the compounds were perfectly docked into the active site of ERα. The unsubstituted compound 4a, the p-chloro substituted compound 4b and the p-fluro-substituted compound 4g were docked successfully in the co-activator grove of protein. The docking pose of compound 4a was shown in Figure 4, which forms a hydrogen bond with Asp351 (carboxyl oxygen atom) with tertiary nitrogen of dimethylamine which is essential for estrogen receptor modulatory activity. The p-chloro substitution in compound 4b form $\pi-\pi$ stacking interaction between amino acid Phe404 was also observed. Figure 4 shows the docking poses of 4a and 4b.

CONCLUSION

In summary, a series of *N*-aryl-2-pyrazolines derivatives were synthesized and evaluated for their binding activity with ER receptor and modulate it. The derivatives with electronegative substitution on the benzylidene motif turned out to be ineffective in the *in vitro* assays performed for evaluating the binding activity with ER. The derivative with *p*-chloro substitution on the benzylidene motif (compound 4b) tends to bind effectively with the ERα; its ability to bind with the receptor was also substantiated by *in vivo* activity.

ACKNOWLEDGEMENT

The authors are thankful to Tata Memorial Centre-Advanced Centre for Treatment, Research and Education in Cancer (ACTREC) Kharghar, Navi Mumbai for *in vitro* anti-breast cancer activity. The authors are also thankful to SAIF, Panjab University, Chandigarh, India for providing spectroscopic facilities.

Conflict of Interest

The authors confirm that this article's content has no conflict of interest.

Funding Support

The authors declare that they have no funding support for this study.

REFERENCES

[1] American Cancer Society. Cancer Facts & Figures. *Atlanta: American Cancer Society*, pages 3–4, 2019.

[2] L Liu, Z Tang, C Wu, X Li, A Huang, X Lu, Q You, and H Xiang. Synthesis and Biological evaluation of 4,6-diaryl-2-pyrimidinamine derivatives as anti-breast cancer agents. *Bioorg. Med. Chem. Lett*, 28(6):1138–1142, 2018.

[3] F Bray, J Ferlay, I Soerjomataram, R L Siegel, L A Torre, and A Jemal. Global cancer statistics 2018: GLOBOCAN estimates of incidence and mortality worldwide for 36 cancers in 185 countries. *CA Cancer J. Clin*, 68(6):394–424, 2018.

[4] I Ahmad Shagufta. Tamoxifen a pioneering drug: An update on the therapeutic potential of tamoxifen derivatives. *Eur. J. Med. Chem*, 143:515–531, 2018.

[5] J M Gross and D Yee. How does the estrogen receptor work? *Breast Cancer Res*, 4(2):62–64, 2002.

[6] M Jia, K D Wright, and J A Gustafsson. Estrogen receptor alpha and beta in health and disease. Best Practice & Research. *Clinical Endocrinology & Metabolism*, 29(4):557–568, 2015.

[7] P N Dube, Y B Thombare, and V A Chatpalliwar. Design and Synthesis of Novel Chalcone-Phenylpyranone Derivatives as Estrogen Receptor Modulators. *Proceedings MDPI*, 9(1):1–7, 2019.

[8] S Fustero, M S Rosello, P Barrio, and A S Fuentes. From 2000 to Mid-2010: A Fruitful Decade for the Synthesis of Pyrazoles. *Chem. Rev*, 111(11):6984–7034, 2011.

[9] C Zhuang, W Zhang, C Sheng, W Zhang, C Xing, and Z Miao. Chalcone: A Privileged Structure in Medicinal Chemistry. *Chem. Rev*, 117(12):7762–7810, 2017.

[10] E A Ariazi, G M Clark, and J E Mertz. Estrogen-related receptor alpha and estrogen-related receptor gamma associate with unfavorable and favorable biomarkers, respectively, in human breast cancer. *Cancer Res*,

62(22):6510–6518, 2002.

[11] S Mandal and J R Davie. An integrated analysis of genes and pathways exhibiting metabolic differences between estrogen receptor-positive breast cancer cells. *BMC Cancer*, 7:181–181, 2007.

[12] P N Dube, M N Waghmare, and S N Mokale. Synthesis, In-vitro & In-vivo biological evaluation and Molecular Docking Analysis of Novel 3-(3-oxo-substituted phenyl-3-)4-(2-(piperidinyl)ethoxy)phenyl)propyl)-2Hchromen-2-one Derivatives as Anti-breast Cancer Agents. *Chem. Biol. Drug Des*, 87(4):608–617, 2016.

[13] P N Dube and S N Mokale. Design and Synthesis of Some Novel Estrogen Receptor Modulators as Anti-Breast Cancer Agents: In Vitro & In Vivo Screening, Docking Analysis. *Anti-cancer Agents Med. Chem*, 16(11):1461–1467, 2016.

[14] P Skehan, R Storeng, D Scudiero, A Monks, J Mcmohan, D Vistica, T W Jonathan, J T Warren, H Bokesch, S Kenny, and M R Boyd. New colorimetric cytotoxicity assay for anticancer-drug screening. *J. Natl. Cancer Inst*, 82(13):1107–1112, 1990.

[15] P N Dube, N S Sakle, S A Dhawale, S A More, and S N Mokale. Synthesis, Biological Investigation and Docking Study of Novel Chromen Derivatives as Anti- Cancer Agents. *Anti-Cancer Agents in Medicinal Chemistry*, 19(9):1150–1160, 2019.

[16] S N Mokale, A Begum, N S Sakle, V R Shelke, and S A Bhavale. Design, synthesis and anticancer screening of 3-(3-(substituted phenyl) acryloyl)-2H-chromen-2-ones as selective anti-breast cancer agent. *Biomedicine & Pharmacotherapy*, 89:966–972, 2017.

[17] S R Teplitzky, T L Kiefer, Q Cheng, P D Dwivedi, K Moroz, L Myers, M B Anderson, A Collins, J Dai, L Yuan, L L Spriggs, D E Blask, and S M Hill. Chemoprevention of NMU-induced rat mammary carcinoma with the combination of melatonin and 9-cis-retinoic acid. *Cancer Lett*, 168(2):155–163, 2001.

[18] Schrödinger Release. Schrödinger Release 2019-1: Glide, Schrödinger, LLC, New York, 2019.